Anal. Chem. **2009,** *81,* 4308–4311

Nanoholes As Nanochannels: Flow-through Plasmonic Sensing

Fatemeh Eftekhari,[†] Carlos Escobedo,[‡] Jacqueline Ferreira,[§,||] Xiaobo Duan,[⊥] Emerson M. Girotto,[||] Alexandre G. Brolo,*[,§] Reuven Gordon,*[,†] and David Sinton*[,‡]

Electrical and Computer Engineering, Mechanical Engineering, and Chemistry, University of Victoria, Victoria, British Columbia, Canada, Universidade Estadual de Maringa, Maringa, PR, Brazil, and British Columbia Cancer Agency, Trev & Joyce Deeley Research Centre, Victoria, British Columbia, Canada

We combine nanofluidics and nanoplasmonics for surface-plasmon resonance (SPR) sensing using flow-through nanohole arrays. The role of surface plasmons on resonant transmission motivates the application of nanohole arrays as surface-based biosensors. Research to date, however, has focused on dead-ended holes, and therefore failed to harness the benefits of nanoconfined transport combined with SPR sensing. The flow-through format enables rapid transport of reactants to the active surface inside the nanoholes, with potential for significantly improved time of analysis and biomarker yield through nanohole sieving. We apply the flow-through method to monitor the formation of a monolayer and the immobilization of an ovarian cancer biomarker specific antibody on the sensing surface in real-time. The flow-through method resulted in a 6-fold improvement in response time as compared to the established flow-over method.

Ordered arrays of nanoscale holes in metal films exhibit unique optical transmission characteristics at resonant wavelengths.[1,2] The role of surface plasmon resonance (SPR) on resonant transmission through nanohole arrays has motivated their application as surface-based biosensors.[3] As compared to common SPR sensing, nanohole arrays present many advantages, including a smaller foot-print, lower limits of detection, denser integration, multiplexing, and collinear optical detection.[4−8] These characteristics of nanohole array-based sensors make them particularly well-suited to planar integration with microfluidics in an on-chip format.

Integration of nanohole arrays in microfluidic platforms has evolved rapidly from single-array, single-channel arrangements that facilitate fluid delivery and optical access, to multiplexed arrays of nanohole arrays and service fluidics. A detailed review of recent progress in this area is available elsewhere.[5] The density to which individual nanohole array sensors may be integrated in plane is highlighted in a recent report of 10^7 sensors per square centimeter.[9] There have also been many developments in the supporting instrumentation and device-level integration of nanohole array based sensors.[10] Most notably, for large scale sensor arrays it is more efficient to monitor transmission intensity changes at a set input wavelength[4,6,8] as opposed to detecting peak shifts in broadband transmission spectra. Transmission intensity measurements may be made using commercial cameras or other detector arrays in parallel and real-time.[8] In all of the developments to date, the nanohole array has been employed in a flow-over format,[5] and thus from a transport perspective these nanostructured sensors showed no inherent advantages over microsized surface based sensor technologies.

As a chemical and biological sensor technology, the sensitivity and limit of detection of nanohole array sensors are of central importance. With improved external optics, the sensitivity of nanohole arrays has been demonstrated to be similar to traditional Kreschmann configuration SPR.[11] With respect to limit of detection, we recently compared the sensitivity of a typical nanohole array to that of an otherwise similar array with a silicon oxide layer blocking access to the top surface. The sensitivities of both devices were comparable; however, the in-hole sensing enabled a 5-fold reduction in the sensing area and the detection of proteins in the attomole range.[12] With the benefits of exclusive in-hole sensing established, effective transport of analytes to the in-hole surface presents an opportunity to harness the rapid cross-stream diffusion characteristic of nanofluidic transport. Research to date involving nanohole arrays has focused on dead-ended holes, and therefore failed to harness the potential benefits from rapid

* To whom correspondence should be addressed. E-mail: agbrolo@uvic.ca (A.G.B.), rgordon@uvic.ca (R.G.), dsinton@uvic.ca (D.S.).
[†] Electrical and Computer Engineering, University of Victoria.
[‡] Mechanical Engineering, University of Victoria.
[§] Chemistry, University of Victoria.
[||] Universidade Estadual de Maringa.
[⊥] Trev & Joyce Deeley Research Centre.

(1) Ebbesen, T. W.; Lezec, H. J.; Ghaemi, H. F.; Thio, T.; Wolff, P. A. *Nature* **1998**, *391*, 667–669.
(2) Genet, C.; Ebbesen, T. W. *Nature* **2007**, *445*, 39–46.
(3) Brolo, A. G.; Gordon, R.; Leathem, B.; Kavanagh, K. L. *Langmuir* **2004**, *20*, 4813–4815.
(4) Yang, J. C.; Ji, J.; Hogle, J. M.; Larson, D. N. *Nano Lett* **2008**, *8*, 2718–2724.
(5) Gordon, R.; Sinton, D.; Kavanagh, K. L.; Brolo, A. G. *Acc. Chem. Res.* **2008**, *41*, 1049–1057.
(6) Lesuffleur, A.; Im, H.; Lindquist, N. C.; Lim, K. S.; Oh, S. H. *Opt. Express* **2008**, *16*, 219–224.
(7) Sharpe, J. C.; Mitchell, J. S.; Lin, L.; Sedoglavich, H.; Blaikie, R. J. *Anal. Chem.* **2008**, *80*, 2244–2249.
(8) Ji, J.; O'Connell, J. G.; Carter, D. J. D.; Larson, D. N. *Anal. Chem.* **2008**, *80*, 2491–2498.
(9) Lindquist, N. C.; Lesuffleur, A.; Im, H.; Oh, S.-H. *Lab Chip* **2009**, *9*, 382–387.
(10) Sinton, D.; Gordon, R.; Brolo, A. G. *Microfluid. Nanofluid.* **2008**, *4*, 107–116.
(11) Tetz, K. A.; Pang, L.; Fainman, Y. *Opt. Lett.* **2006**, *31*, 1528–1530.
(12) Ferreira, J.; Santos, M. J. L.; Rahman, M. M.; Brolo, A. G.; Gordon, R.; Sinton, D.; Girotto, E. M. *J. Am. Chem. Soc.* **2009**, *131*, 436–437.

10.1021/ac900221y CCC: $40.75
Published on Web 05/01/2009

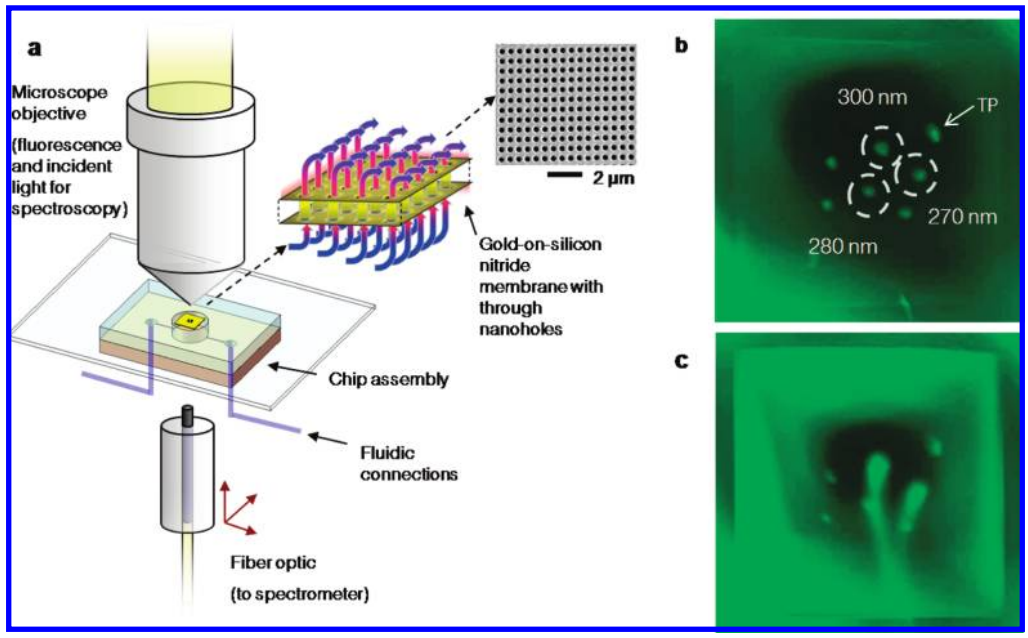

Figure 1. Flow-through nanohole arrays. (a) Schematic of the optical and fluidic test setup employed for both fluorescence tests and transmission spectroscopy. (b) Fluorescence image of the gold film with nanohole arrays, prior to the application of fluid pressure. The location of the arrays is indicated from the emission of the fluorescein solution on the underside. Arrays were 15 × 15 μm^2, with periodicities of 450 nm and hole diameters of 300, 280, 270 nm (as indicated), as well as 260 and 250 nm and the test pattern (TP). (c) Fluorescence image showing a dye buffer solution streaming from the three largest diameter arrays with 70 kPa applied pressure. The extent of the square silicon support frame (500 × 500 μm^2) becomes apparent as the fluid pressure deforms the membrane upward. (See Supporting Information, Movie 1).

diffusion at nanoscales and from solution sieving using nanostructures.[13,14]

In this paper, we demonstrate nanohole arrays with through-holes as flow-through SPR sensing elements. This paper describes the fabrication, microfluidic integration, and the application of flow-through nanohole array based sensors to chemical sensing. The flow-through array sensor introduced in this work combines the benefits of nanohole array based sensing with nanoconfined transport through the combination of nanofluidics and nanoplasmonics.

MATERIALS AND METHODS

Fabrication of the Nanohole Arrays. The circular nanohole arrays were fabricated by focused-ion beam (FIB) milling through a 100 nm thick gold films thermally evaporated on free-standing 100 nm Si_3N_4 with a 5 nm thick chromium adhesion layer. The evaporation was done commercially (EMF, Ithaca, NY). A variety of milling parameters were attempted in an effort to determine appropriate milling parameters for fabricating through-holes. For the arrays that demonstrated through-hole transport, the general milling parameters were as follows: the gallium ion beam was set to 30 keV for milling with a beam current of 50 pA, the typical beam spot size was 10 nm, and the dwell time of the beam at one pixel was 4 ms. The arrays consisted of 30 × 30 nanoholes with periodicities between 450−700 nm. Although several membranes were fabricated, the results from two (varying periodicity and varying hole-diameter) are reported in this work. In addition to SEM imaging, fabricated nanoholes were characterized by energy dispersive X-ray spectroscopy (EDX) and TEM imaging. These techniques were used to confirm the milling process, and specifically the extent of the milling through the silicon nitride. Observed transport and through-hole sensing, however, were the ultimate metrics employed to assess the fabricated sensors.

Fabrication of the Microfluidics and Flow Setup. The gold and silicon nitride film, immobilized on a silicon frame, was integrated into a poly(dimethylsiloxane) (PDMS) chip fabricated by soft-lithographic rapid prototyping.[15] Fluids were provided to the chip through syringe pumps; however, much care was required in the setup and running of the flow-through experiments to facilitate wetting of the nanoholes and avoid spurious pressure forces sufficient to rupture the membrane. Detailed information on the fabrication and assembly of the integrated chip and the experimental setup is provided in the Supporting Information.

Chemicals. Ethanol anhydrous, and 11-mercaptoundecanoic acid (MUA, 95%) were purchased from Sigma-Aldrich. Dithiobis-(succinimidyl undecanoate) (DSU, 92.7%) was purchased from Dojindo Laboratories. Sodium chloride (99%), sodium phosphate dibasic (99%), and potassium chloride (99%) were purchased from ACP, and fluorescein was purchased from Invitrogen. Pared box gene (PAX8) protein was provided by the Antibody Research Unit of the British Columbia Cancer Agency (Canada).

RESULTS AND DISCUSSION

Fabrication and Imaging of Flow-Through Nanohole Transport. Figure 1a shows a schematic of the suspended nanohole array integrated with microfluidics, and the setup for microscopic imaging and fiber-based transmission spectroscopy. Integrated

(13) Chou, I.-H.; Benford, M.; Beier, H. T.; Cote, G. L.; Wang, M.; Jing, M.; Kameoka, J. *Nano Lett.* **2008**, *8*, 1729–1735.
(14) Liang, X. G.; Chou, S. Y. *Nano Lett.* **2008**, *8*, 1472–1476.
(15) Duffy, D. C.; McDonald, J. C.; Schueller, O. J. A.; Whitesides, G. M. *Anal. Chem.* **1998**, *70* (23), 4974–4983.

service microfluidics delivered solutions and facilitated control of the solution pressure on the underside (Si_3N_4 side) of the membrane. Figure 1b shows a microscope image of six arrays of nanoholes, and a test pattern (TP) as lighter regions near the center of the image. Figure 1c shows the flow-through visualization using fluorescein. The dye was injected from the Si_3N_4 side of the template, and the image of the Au side showed pronounced streaming through the largest nanoholes under applied pressure (see Supporting Information, Movie 1). Of the six arrays fabricated with periodicity p = 450 nm, and different milling parameters, three arrays showed flow-through, corresponding to the hole diameters indicated in Figure 1b. The lack of apparent flow through three arrays was attributed to a combination of smaller hole diameter and insufficient dwell times (i.e., the milling time used to fabricate those arrays did not allow the formation of through holes). With the applied pressure of 10 psi (70 kPa), the total flow rate through the three arrays was estimated to be 5 μL/min, which is compatible with existing microfluidic delivery systems.[16] The arrays showed reversible deflection on the order of 30 μm under the applied pressure. The same SPR spectrum was obtained form the arrays before and after extensive flow-through tests, indicating that the nanostructured arrays were not functionally damaged. It is interesting to note that nanoporous Si membranes as thin as 15 nm have been shown to withstand pressure differentials on the order of one atmosphere.[17] Silicon nitride membranes in particular have been demonstrated previously as suitable substrates with which to observe resonant transmission through nanohole arrays.[18]

SPR Sensing Using Flow-Through Delivery of Analyte. Figure 2a shows the optical transmission spectra for the arrays of nanoholes in air (refractive index, n = 1.0008) and in ethanol (n = 1.3587). The spectral shift indicates the sensitivity of the resonant transmission to bulk refractive index.[19,20] In air, the SPR peak is at 575 nm, but in ethanol it shifted to λ = 625 nm (periodicity, p = 500 nm). The SPR is dominated from the exposed gold surface as the response from the gold−silicon nitride interface is expected to be damped by the chromium adhesion layer.[21] A sensitivity of 324 nm RIU^{-1} was found using glucose solutions with fine refractive index gradations between 1.3324 and 1.3568. This sensitivity is similar to previous nanohole SPR.[3,20] We note that flow-through sensing is compatible with recent strategies to increase nanohole SPR sensitivity relative to that of commercial SPR.[11]

The efficacy of flow-through nanohole arrays in the detection of surface adsorption events was tested. The solution containing the testing adsorbate was introduced in the microchamber in contact with the Si_3N_4 surface. In this way the sensor response to adsorption at the active gold surface is observed only after flow-through hole transport. The well-known self-assembly of a monolayer of mercaptoundecanoic acid (MUA) on a gold surface followed.[22] The surface-adsorption was monitored in real-time by the shift in the λ = 625 nm peak as a 500 nM ethanolic solution of MUA streamed through the nanohole arrays from the Si_3N_4 side (p = 500 nm array). This MUA concentration resulted in adsorption time scales that enabled accurate timing of the experiments and negligible peak shift response from the bulk liquid. The real-time spectral red-shift caused by the MUA adsorption is shown in Figure 2b. The SPR peak position approached a steady state value indicating that the self-assembled monolayer approached completion. A similar test was conducted in flow-over format to compare the response

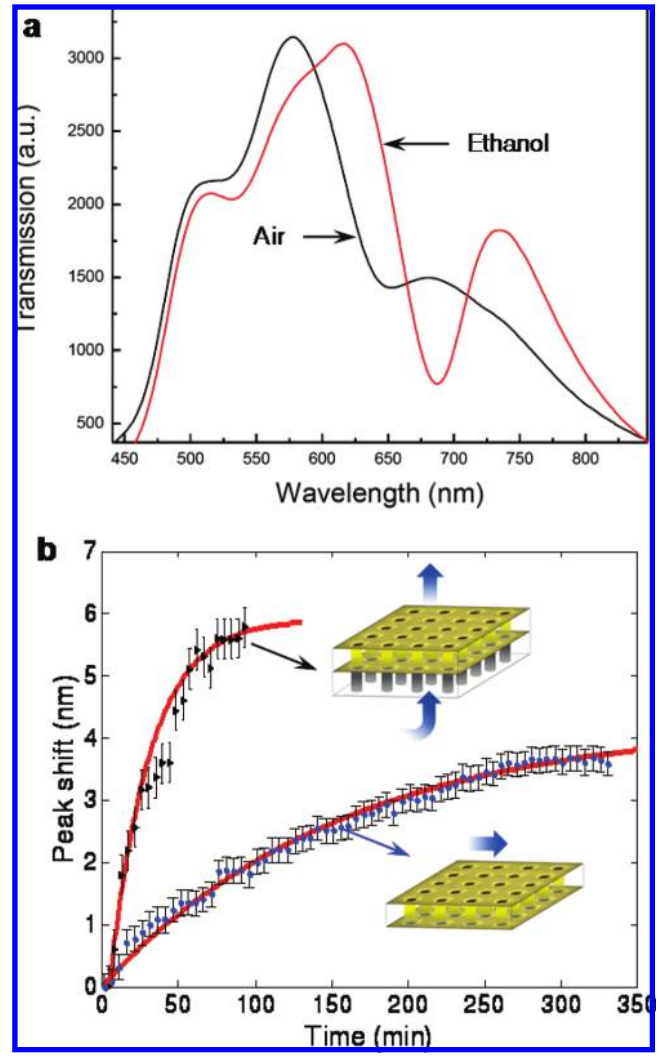

Figure 2. Response of flow-through nanohole arrays to bulk refractive index and surface adsorption: (a) Transmission spectra for air (n = 1.0008) and ethanol (n = 1.3587) in an array of periodicity, p = 500 nm; and (b) comparison of response to surface adsorption achieved with flow-over and flow-through formats as indicated inset. Measured peak shift (625 nm peak) is plotted as a function of time during flow through/over of an ethanol/MUA solution. As indicated in the inset, the flow-through sensor is operated with flow from the nonparticipating silicon nitride side to the active gold surface. The flow-through case results in a characteristic rate constant of k_{abs} = 3.8 × 10^{-2} min^{-1} as compared to k_{abs} = 6.4 × 10^{-3} min^{-1} for the flow-over case.

(16) Whitesides, G. M. *Nature* **2006**, *442*, 368–373.
(17) Striemer, C. C.; Gaborski, T. R.; McGrath, J. L.; Fauchet, P. M. *Nature* **2007**, *445*, 749–753.
(18) Grupp, D. E.; Lezec, H. J.; Ebbesen, T. W. *Appl. Phys. Lett.* **2000**, *77*, 1569–1571.
(19) Krishnan, A.; Thio, T.; Kim, T. J.; Lezec, H. J.; Ebbesen, T. W.; Wolff, P. A.; Pendry, J.; Martin-Moreno, L.; Garcia-Vidal, F. J. *Opt. Commun.* **2001**, *200*, 1–7.
(20) De Leebeeck, A.; Kumar, L. K. S.; De Lange, V.; Sinton, D.; Gordon, R.; Brolo, A. G. *Anal. Chem.* **2007**, *79*, 4094–4100.
(21) Genet, C.; van Exter, M. P.; Woerdman, J. P. *Opt. Commun.* **2003**, *225*, 331–336.
(22) Love, J. C.; Estroff, L. A.; Kriebel, J. K.; Nuzzo, R. G.; Whitesides, G. M. *Chem. Rev.* **2005**, *105*, 1103–1169.

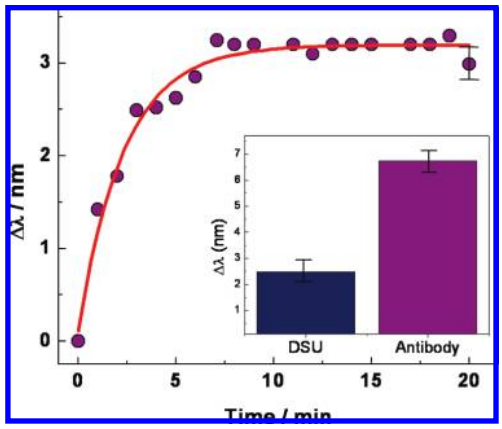

Figure 3. Response of flow-through nanohole arrays to sequential adsorption (periodicity of 450 nm). The wavelength versus time plot shows the peak-shift in response to the antibody (PAX8) adsorption, with a representative error bar on the last data point. Inset is a bar graph showing the peak shift in response to the initial DSU monolayer and the total peak shift in response to the DSU and the antibody.

achieved with flow-through sensing to the established flow-over practice. A channel of 50 μm × 2.5 mm cross-section covered the flow-over nanohole array, and the peak-shift was monitored in response to the ethanolic solution of MUA at a flow rate comparable to the flow-through case (~1 μL/min). The results of the flow-over test are also plotted in Figure 2b. The MUA adsorption was fit to a first-order kinetics curve.[23,24] The flow-through exponential fit indicates a characteristic rate constant of $k_{abs} = 3.8 \times 10^{-2}$ min^{-1} as compared to $k_{abs} = 6.4 \times 10^{-3}$ min^{-1} for the flow-over case. These results indicate a 6-fold improvement in the adsorption kinetics by employing nanoholes as nanochannels as compared to the established flow-over method.

Application to Sensing of Cancer Biomarker-Specific Antibody Binding. The label-free detection of cancer markers by SPR requires the immobilization of the antibody and detection through multiple adsorbed layers.[25] Here, the sequential assembly of a monolayer and the cancer biomarker PAX8 specific monoclonal antibody[26] were demonstrated with the flow-through scheme. The goal was to show that the flow-through approach enables the monitoring of multilayer adsorption. Dithiobis(succinimidyl)undecanoate (DSU) was first immobilized at the gold surface by flowing an ethanolic solution of DSU through the nanohole array (p = 450 nm), followed by a rinse step. A SPR shift of about 2.5 nm confirmed the formation of a monolayer of the adsorbed target. A 3.5 μg mL^{-1} (80 nM, with molecular weight of 43 kDa) aqueous solution of PAX8 protein in phosphate buffer solution was then transported through the nanoholes, and the adsorption kinetics were monitored by the SPR peak shift, as plotted in Figure 3. The sensor response shows a rapid increase over 7 minutes followed by a steady state. The PAX8 adsorption to DSU is non-specific and fits to a first order kinetic model, yielding an observable adsorption rate constant of 0.445 min^{-1}. The final relative SPR shifts corresponding to the DSU and the combined DSU/antibody adsorption are shown inset in Figure 3. The observed shifts, on the order of several nanometers, are readily observable with relatively simple infrastructure. These results demonstrate that the flow-through nanohole array based sensors may be employed to detect multiple adsorbed layers.

(23) Karpovich, D. S.; Blanchard, G. J. *Langmuir* **1994**, *10*, 3315–3322.
(24) Peterlinz, K. A.; Georgiadis, R. *Langmuir* **1996**, *12*, 4731–4740.
(25) Shumaker-Parry, J. S.; Aebersold, R.; Campbell, C. T. *Anal. Chem.* **2004**, *76*, 2071–2082.
(26) Bowen, N. J.; Logani, S.; Dickerson, E. B.; Kapa, L. B.; Akhtar, M.; Benigno, B. B.; McDonald, J. F. *Gynecol. Oncol.* **2007**, *104*, 331–337.

CONCLUSION

In summary, we have demonstrated flow-through nanohole array based sensing that combines the benefits of nanofluidics and nanoplasmonics in a single platform. It was shown that nanohole array based sensing may be performed with through nanoholes, or nanochannels, that facilitate enhanced transport of reactants to the active surface. As fluidic elements, the nanohole arrays served to parallelize the resistance and thus fluid handling and control were compatible between the parallel nanochannels and established microfluidic protocols. As optical elements, the nanohole arrays served to detect the adsorption of a monolayer as well as the step-by-step multilayer assembly of biomolecules as required for biosensing applications. A side-by-side comparison with the established flow-over methodology showed a 6-fold improvement in response time using the flow-through approach. Finally, we suggest that the flow-through nanohole arrays as combined plasmonic and fluidic elements exhibit many features that are particularly promising for sensing technologies. These features include a small foot-print, collinear optical detection, co-nanoconfinement of the analyte and the sensing electromagnetic field, enhanced transport through rapid diffusion at nanoscales, and a solution-sieving action for surface based sensing. In addition, the flow-through nanohole array scheme presented here is ideal for in-hole sensing. Exclusive use of the in-hole surface reduces the number of adsorption sites, while providing a large spectral shift, improving the limit of detection into the attomolar range. The flow-through approach greatly enhances transport of analytes to the active area inside the holes. We anticipate that the flow-through nanohole arrays will enable highly integrated, multiplexed, label-free diagnostics for which efficient screening of multiple biomarkers is essential.

ACKNOWLEDGMENT

We gratefully acknowledge funding support for this work from NSERC, CFI, and BCKDF. This collaboration has been facilitated by an NSERC Strategic Projects Grant with the BC Cancer Agency and Micralyne Inc. We thank Paul Wood and Michael Fryer for helpful discussions. We also thank the Government of Canada for the scholarship provided by the Graduate Students' Exchange Program (GSEP) to J.F.

SUPPORTING INFORMATION AVAILABLE

Additional information as noted in the text. This material is available free of charge via the Internet at http://pubs.acs.org.

Received for review January 29, 2009. Accepted April 23, 2009.

AC900221Y